Interacting topological mirror excitonic insulator in one dimension

Lun-Hui Hu,[1,2,*] Rui-Xing Zhang,[3,†] Fu-Chun Zhang,[2,4,5] and Congjun Wu[1]

[1]*Department of Physics, University of California, San Diego, La Jolla, California 92093, USA*
[2]*Kavli Institute of Theoretical Sciences, University of Chinese Academy of Sciences, Beijing 100049, China*
[3]*Condensed Matter Theory Center and Joint Quantum Institute, Department of Physics, University of Maryland, College Park, Maryland 20742-4111, USA*
[4]*CAS Center for Excellence in Topological Quantum Computation, University of Chinese Academy of Sciences, Beijing 100049, China*
[5]*Collaborative Innovation Center of Advanced Microstructures, Nanjing University, Nanjing 210093, China*

(Received 19 August 2020; revised 17 November 2020; accepted 19 November 2020; published 7 December 2020)

We introduce the topological mirror excitonic insulator as a new type of interacting topological crystalline phase in one dimension. Its mirror-symmetry-protected topological properties are driven by exciton physics, and it manifests in the quantized bulk polarization and half-charge modes on the boundary. And the bosonization analysis is performed to demonstrate its robustness against strong correlation effects in one dimension. Besides, we also show that Rashba nanowires and Dirac semimetal nanowires could provide ideal experimental platforms to realize this new topological mirror excitonic insulating state. Its experimental consequences, such as quantized tunneling conductance in the tunneling measurement, are also discussed.

DOI: 10.1103/PhysRevB.102.235115

I. INTRODUCTION

The conceptual revolution of topological physics [1–14] in solids has changed our way of classifying phases of matters, which has had a great impact on experimental discoveries of topological insulators (TIs) [15–18]. By definition, a time-reversal-invariant TI is characterized by the nontrivial $\mathbb{Z}_2$ band topology and the resulting gapless boundary modes, both of which are protected by time-reversal symmetry [19–21]. This symmetry protection [13], upon which only the $\mathbb{Z}_2$ topological invariant is well defined, distinguishes TIs from earlier examples such as integer/fractional quantum Hall systems. And it leads to the concept of the symmetry-protected topological (SPT) state [22]. The framework of symmetry-protected band topology has been successfully extended from time-reversal symmetry to crystalline topological systems protected by space-group symmetries [23–28], magnetic-group symmetries [29–31], and space-time symmetries [32,33]. Remarkable progress has been made along this direction, which has led to the theoretical predictions and experimental discoveries of the crystalline topological phase in SnTe [34], $Pb_{1-x}Sn_xSe$ [35], KHgSb [36,37], and, recently, $MnBi_{2n}Te_{3n+1}$ [38–45].

Meanwhile, there has been great interest in exploring the fate of SPT phases under strong electron correlations [46–48]. For example, interaction effects could (i) fundamentally change the topology by breaking symmetries spontaneously [49–52] or alter the topological classification of SPT states [53–57] and (ii) enable new topological phases which do not exist in the free fermion limit [51,58–69]. However, little is known about how to realize interacting SPT states in experiments [69–76] as well as how to detect them, especially in systems with crystalline-symmetry protection.

In this work, we introduce the topological mirror excitonic insulator (TMEI) as a new type of interacting crystalline topological state in one dimension and propose to experimentally realize this novel topological state in two physical systems, namely, Rashba nanowires [77–79] and Dirac semimetal nanowires [80–82]. The TMEI is characterized by a quantized bulk charge polarization and a mirror-protected boundary half-charge mode when interaction-induced excitonic order is formed. To fully incorporate the interaction effects in one dimension, we construct an effective field theory description of the TMEI in the Rashba nanowire system by applying Abelian bosonization technique, which shows the robustness of the TMEI beyond the mean-field level. This allows us to map out the topological phase diagram and clarify the necessary conditions for realizing the TMEI phase. Experimentally, we propose quantized tunneling conductance as the smoking-gun signal for the TMEI, which clearly distinguishes the TMEI phase from other states.

II. MODEL HAMILTONIAN

The minimal system for one-dimensional (1D) exciton physics consists of one electron band and one hole band [83]. Such two-channel systems can be realized in (i) a double-wire setup with one n-type nanowire (electron doping) and a p-type nanowire (hole doping) and (ii) a single quantum wire with two conducting channels that have opposite effective masses. In this paper, we focus on the TMEI physics in the double-nanowire setup and briefly discuss its realization in a single Dirac semimetal nanowire.

*l1hu@physics.ucsd.edu
†ruixing@umd.edu

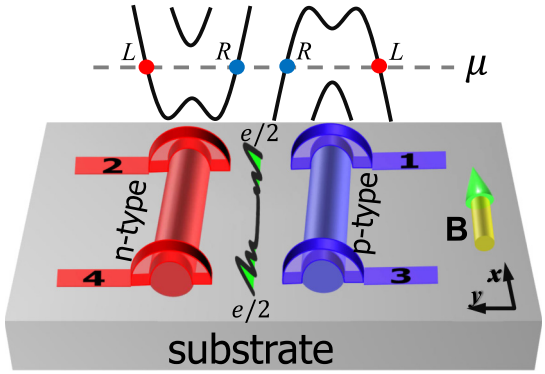

FIG. 1. Schematics of two coupled nanowires for the topological mirror excitonic insulator. The left, red wire is n-type and the right, blue wire is p-type. An in-plane magnetic field $\vec{B}$ is applied along the $\hat{x}$ direction. The top panel shows electron or hole dispersions for n-type (left) and p-type (right) wires in Eq. (1), respectively, with only one left (L)-moving and one right (R)-moving electron or hole at a chemical potential μ illustrated by the dashed horizontal line. A topological mirror excitonic insulator may be realized when the interaction between two nanowires is introduced, and half-charge modes are localized at the ends.

The double-nanowire system on an insulating substrate is illustrated in Fig. 1. We consider a $\mathbf{k}\cdot\mathbf{p}$ Hamiltonian [84] to describe the low-energy band structure of the double Rashba nanowires under a magnetic field along the wire direction x,

$$\mathcal{H}_0 = \epsilon(k_x) + \big(m_0 k_x^2 - \mu\big)\sigma_0\tau_z + v k_x \sigma_y \tau_0 + h\sigma_x\tau_0, \qquad (1)$$

in which Pauli matrices τ_i and σ_i denote the wire and spin degrees of freedom, respectively, $\epsilon(k_x) = \delta\mu + \delta m k_x^2 m_0$ is the inverse of the effective mass, μ is the chemical potential, v characterizes the Rashba spin-orbit coupling, and h represents the Zeeman splitting energy induced by an applied magnetic field $\mathbf{B}$. In the strained nanowires, $\delta m \to 0$ can be achieved [85]. Here we assume that m_0, v, and h are all positive, and there is a high tunneling barrier between the wires that suppresses the single-electron tunneling between the wires. Nevertheless, pair hopping processes still exist as a result of interwire interactions. When $\mathbf{B}$ is aligned along the wires ($\hat{x}$ direction), and the Hamiltonian, Eq. (1), has mirror symmetry, $M_x = i\sigma_x \cdot P$, where P maps x to $-x$ [86]. In fact, M_x is the lattice symmetry of the Rashba wires, which holds for both the lattice and the continuum limits.

III. EXCITONS AND TOPOLOGY

To examine the band topology stemming from the exciton physics, we consider an interwire interaction,

$$\mathcal{H}_{\rm int} = \int dx\, \hat{n}_e(x)\hat{n}_h(x), \qquad (2)$$

where $\hat{n}_i(x) = \sum_{\alpha=\uparrow,\downarrow} c^\dagger_{i\alpha}(x)c_{i\alpha}(x)$ is the density operator with $i = \{e, h\}$. The excitonic orders [87–91] may introduce an energy gap in the double-wire system, in favor of the excitonic state energetically. Based on the representations of M_x, there are two classes:

$$\begin{aligned} &\text{mirror-even orders,} \quad \Delta_{\rm even} = \sigma_{0(x)}\tau_{x(y)};\\ &\text{mirror-odd orders,} \quad \Delta_{\rm odd} = \sigma_{y(z)}\tau_{x(y)}. \end{aligned} \qquad (3)$$

As a result, the mean-field Hamiltonian is given by

$$\mathcal{H}_{\rm MF} = \mathcal{H}_0 + H_{\rm ec}, \qquad (4)$$

where $\mathcal{H}_0$ is the noninteracting Hamiltonian in Eq. (1) and $H_{\rm ec}$ is for the excitonic orders in Eq. (3). To show the gap opening by $H_{\rm ec}$, we take it as a perturbation. In the absence of $H_{\rm ec}$, the eigenstates at $k_x = 0$ are

$$\begin{aligned} |h+\mu\rangle &= [1,1,0,0]^{\rm T}/\sqrt{2} \quad \text{and} \quad m_x = +i,\\ |h-\mu\rangle &= [0,0,1,1]^{\rm T}/\sqrt{2} \quad \text{and} \quad m_x = +i,\\ |-h+\mu\rangle &= [1,-1,0,0]^{\rm T}/\sqrt{2} \quad \text{and} \quad m_x = -i,\\ |-h-\mu\rangle &= [0,0,1,-1]^{\rm T}/\sqrt{2} \quad \text{and} \quad m_x = -i, \end{aligned} \qquad (5)$$

where we assume that $-h < \mu < h$, and m_x is the eigenvalue of the mirror symmetry M_x. By perturbation theory, we find that mirror-even order parameters tend to lower the eigenenergy of the state $|h-\mu\rangle$, while they increase the eigenenergy of the state $|-h+\mu\rangle$. The closing and reopening of the bulk gap indicate that there is a topological phase transition. More explicitly, the bulk dispersion is

$$E_\pm = \delta\mu \pm \big|h \pm \sqrt{\mu^2 + \Delta_0^2}\big|, \qquad (6)$$

and it shows gap closing when $h = \sqrt{\mu^2 + \Delta_0^2}$, indicating that a topological phase transition can be tuned by the external magnetic field. Moreover, the condition for the TMEI phase is

$$h > \sqrt{\mu^2 + \Delta_0^2} \quad \text{with} \quad \Delta_0 \neq 0, \qquad (7)$$

where Δ_0 denotes the amplitude of the mirror-even excitonic orders. Given the TMEI condition, we note that the electron and hole bands are "inverted" near the Fermi level to trigger the nontrivial band topology. This is shown in Fig. 1, where we plot both bands for electron and hole nanowires in the $\Delta_0 \to 0$ limit. As for the mirror-odd orders, they are trivial since they always increase the bulk gap. Namely, they generally spoil M_x and do not lead to nontrivial topology in one dimension.

With mirror-even orders, we can define a quantized bulk electric polarization $\mathcal{P}$ [92–94] to characterize the bulk topology,

$$\mathcal{P} = \frac{i}{2\pi}\sum_n \oint dk_x \langle u_n(k_x)|\partial_{k_x}|u_n(k_x)\rangle, \qquad (8)$$

where $|u_n(k_x)\rangle$ is the Bloch wave function with an occupied-band index n. Crucially, M_x enforces that $\mathcal{P}$ is quantized to an integer multiple of $1/2$ (i.e., 0 or $\frac{1}{2}$ since $\mathcal{P}$ is well defined modulo 1). $\mathcal{P}$ can be numerically calculated within mean-field theory, and the results are shown in Fig. 2, from which we find that only the system with mirror symmetry can be topological. Also, $\mathcal{P} = \frac{1}{2}$ for the TMEI phase, and $\mathcal{P} = 0$ for the topological trivial phase.

To drive the TMEI phase with $\mathcal{P} = \frac{1}{2}$ into a trivial phase (or a vacuum state) with $\mathcal{P} = 0$, the system must undergo a bulk

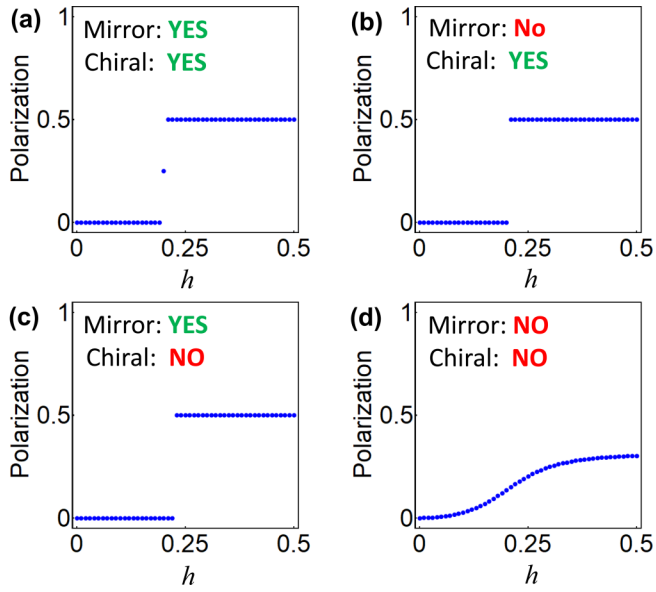

FIG. 2. The Zak phase in different states. (a) Both mirror and chiral symmetries are preserved. (b) Mirror symmetry is broken but chiral symmetry is preserved. (c) Mirror symmetry is preserved but chiral symmetry is broken. (d) Both mirror and chiral symmetries are broken.

gap closing process, which manifests itself as a topological phase transition. With an open boundary condition, one can easily check that the system hosts one localized half-charge mode at each end, similar to the case of the Su-Shrieffer-Heeger model. However, the chiral symmetry $\mathcal{C}$ is not often exact in our system; we emphasize that the mirror-enforced boundary half-charge is more fundamental and robust than the $\mathcal{C}$-protected boundary zero mode in our TMEI phase.

IV. BOSONIZATION AND PHASE DIAGRAM

Next, we establish a Luttinger liquid theory to show that the TMEI physics remains robust when interaction effects are considered, which is beyond the mean-field theory. Since there is a pair of counter-propagating modes in each wire (see Fig. 1), we follow the standard mapping from the fermion fields $\Psi_{i,s}$ to the chiral boson fields $\chi_{i,s}$ by

$$\Psi_{i,s} = \frac{\eta_{i,s}}{\sqrt{4\pi a}} e^{is\sqrt{4\pi}\chi_{i,s}}, \tag{9}$$

where a is the lattice constant and $\eta_{i,s}$ are Klein factors [95,96]. Here the wire index $i = \{e, h\}$ labels the n-/p-type nanowire and $s = \pm$ denotes the right-/left-moving fermion modes.

It is convenient to define the dual boson fields as $\phi_i = \chi_{i,R} + \chi_{i,L}$ and $\theta_i = \chi_{i,R} - \chi_{i,L}$. Then the fermionic density operators are given by $\rho_{i,s} = \frac{1}{\sqrt{\pi}}\partial_x \chi_{i,s}$. We first consider the intrawire density-density interaction $g_1 \rho_{i,L}\rho_{i,R}$ and the interwire density-density interaction $g_2(\rho_{e,R}\rho_{h,L} + \rho_{e,L}\rho_{h,R})$, which are known to renormalize the Fermi velocities and Luttinger parameters. For simplicity, we assume that the bare Fermi velocities in these two nanowires are equal. We denote $\phi_\pm = (\phi_e \pm \phi_h)/\sqrt{2}$ and $\theta_\pm = (\theta_e \pm \theta_h)/\sqrt{2}$ and obtain a renormalized free boson model [97–99], which captures the low-energy physics,

$$\mathcal{H}_0 = \frac{v_\pm}{2}\int dx\left[\frac{1}{K_\pm}(\partial_x\phi_\pm)^2 + K_\pm(\partial_x\theta_\pm)^2\right], \tag{10}$$

where $v_\pm = \sqrt{(v_F + (g_1 \pm g_2)/2\pi)(v_F - (g_1 \pm g_2)/2\pi)}$ and $K_\pm = \sqrt{(v_F - (g_1 \pm g_2)/2\pi)/(v_F + (g_1 \pm g_2)/2\pi)}$. Then we include symmetry-allowed and momentum-conserved scattering processes that arise from two-body anharmonic interactions [100], which lead to the Hamiltonian $\mathcal{H} = \mathcal{H}_0 + \mathcal{H}_{\rm int}$, where

$$\mathcal{H}_{\rm int} = \int dx[\alpha_1 \cos(2\sqrt{2\pi}\phi_+) + \alpha_2 \cos(2\sqrt{2\pi}\theta_-)]. \tag{11}$$

Here the first ϕ_+-mass term is valid when a pair of "inverted bands" is formed and the chemical potential is around the energy of the band crossings; the second θ_--mass term describes the interwire pair hopping process. Notably, the ϕ_+-mass term is absent in usual general nanowires with only electronlike (or holelike) bands. In particular, the relevance of the cosine terms can be evaluated by the renormalization-group (RG) equation $d\alpha_i/d\ln\lambda = [1 - \Delta_{\rm sd}(\alpha_i)]\alpha_i$, where the scaling dimensions (sd) of the coupling constants are

$$\Delta_{\rm sd}(\alpha_1) = K_+, \quad \Delta_{\rm sd}(\alpha_2) = \frac{1}{K_-}. \tag{12}$$

Thus, under the RG, we find that α_1 is relevant when $K_+ < 1$, while α_2 is relevant for $K_- > 1$. For the whole Hamiltonian $\mathcal{H} = \mathcal{H}_0 + \mathcal{H}_{\rm int}$, the phase diagram is determined by the Luttinger parameters $K_\pm$ (or equivalently $g_{1,2}$).

We first note that the system remains gapless when $K_+ > 1$. In particular, as for $K_- > 1$, interwire pairhopping processes are greatly promoted. This gaps out the antibonding sector and further leads to number-conserving Majorana physics, which has been intensively discussed in the literature [82,101,102]. This phase is denoted TSC in the phase diagram in Fig. 3(a). On the contrary, when $K_- < 1$, both antibonding and bonding sectors remain gapless. This represents a gapless Luttinger liquid state [LL_b in Fig. 3(a)]. Similarly, a Luttinger liquid state, LL_a, arises for $K_\pm < 1$ since only the bonding sector is trivially gapped. In this case, the antibonding sector could

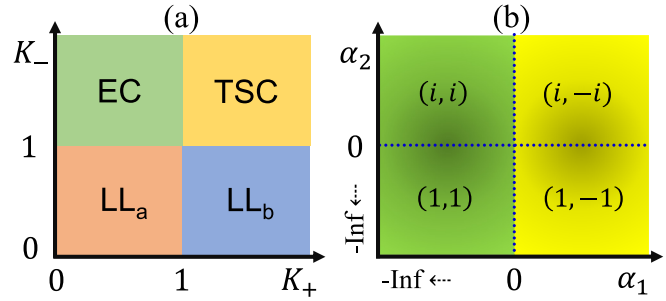

FIG. 3. Phase diagrams. (a) Three phases: the exciton condensation (EC) insulating phase when $K_- > 1$ and $K_+ < 1$; the topological superconducting phase (TSC) phase for $K_\pm > 1$; and the gapless Luttinger liquid ($\mathrm{LL}_{a,b}$) phase when $K_- < 1$. (b) Given by $K_- > 1$ and $K_+ < 1$, the phase diagrams for EC as functions of α_1 and α_2. When $\alpha_1 < 0$, the EC insulating phase breaks mirror symmetry M_x; otherwise, it is mirror symmetric. The expectation values of order parameters $[\Delta_{\rm ex}^{(1)}, \Delta_{\rm ex}^{(2)}]$ are shown in each quarter.

also be trivially gapped due to the pining of the ϕ_--mass term, which is induced by the Umklapp scattering when $k_F \to \pi/2$. We discuss this later.

More importantly, we show that the TMEI is achieved when $K_- > 1$ and $K_+ < 1$. Because $\Delta_{\rm sd}(\alpha_1) < 1$ and $\Delta_{\rm sd}(\alpha_2) < 1$, those cosine terms with $\alpha_{1,2}$ will flow to the strong-coupling limit under the RG. As a result, both θ_- and ϕ_+ will be pinned to the semiclassical values. When the system becomes gapped, we find a set of nonvanishing order parameters,

$$\begin{aligned}\Delta_{\rm ex}^{(1)} &\sim \langle \Psi_{e,R}^\dagger \Psi_{h,L}\rangle \sim \langle e^{-i\sqrt{2\pi}\phi_+} e^{-i\sqrt{2\pi}\theta_-}\rangle \neq 0,\\ \Delta_{\rm ex}^{(2)} &\sim \langle \Psi_{e,L}^\dagger \Psi_{h,R}\rangle \sim \langle e^{i\sqrt{2\pi}\phi_+} e^{-i\sqrt{2\pi}\theta_-}\rangle \neq 0,\end{aligned} \tag{13}$$

which imply an excitonic insulating phase. Now, let us analyze the condition for mirror-even excitonic orders. Under M_x, the boson fields are transformed as $\sqrt{4\pi}\phi_e \to -\sqrt{4\pi}\phi_e + 2\beta$, $\sqrt{4\pi}\theta_e \to \sqrt{4\pi}\theta_e + \pi$, $\sqrt{4\pi}\phi_h \to -\sqrt{4\pi}\phi_h - 2\beta$, and $\sqrt{4\pi}\theta_h \to \sqrt{4\pi}\theta_h - \pi$, where β is an unimportant phase factor. Consequently, the mirror symmetry sends $\phi_+ \to -\phi_+$ and $\theta_- \to \theta_- + \sqrt{\pi/2}$. For the excitonic order parameters, we immediately find that $\Delta_{\rm ex}^{(1)} = -\Delta_{\rm ex}^{(2)}$ respects M_x, while $\Delta_{\rm ex}^{(1)} = \Delta_{\rm ex}^{(2)}$ does not. The relative phase difference between $\Delta_{\rm ex}^{(1)}$ and $\Delta_{\rm ex}^{(2)}$ is determined by the sign of the coupling coefficients α_1 and α_2. For example, when $\alpha_{1,2} > 0$, the semiclassical limit is given by $\theta_- = (n_\theta + \frac{1}{2})\sqrt{\frac{\pi}{2}}$ and $\phi_+ = (n_\phi + \frac{1}{2})\sqrt{\frac{\pi}{2}}$. This leads to $\Delta_{\rm ex}^{(1)} = -\Delta_{\rm ex}^{(1)} = i$ and thus respects M_x symmetry. In Fig. 3(b), we map out the phase diagram with respect to α_1 and α_2. Therefore, the system preserves the mirror symmetry M_x when $\alpha_1 > 0$.

To clarify the topological nature of the above mirror-even excitonic insulating physics, it is instructive to map the excitonic orders in the low-energy basis back to the original fermion basis for Eq. (1). We find that the mirror-even case with $\Delta_{\rm ex}^{(1)} = -\Delta_{\rm ex}^{(2)} = 1$ and $\Delta_{\rm ex}^{(1)} = -\Delta_{\rm ex}^{(2)} = i$ are, respectively, equivalent to the mean-field excitonic orders $\sigma_x\tau_y$ and $\sigma_x\tau_x$ in the original basis [see Eq. (3)], which are already known to lead to the TMEI phase.

Furthermore, the topological properties of the TMEI phase can also be understood via the boson theory. Consider an open boundary condition of the system $x < 0$ in Eq. (10) with the end point $x = 0$, so that $x > 0$ is a vacuum with $\phi_\pm = 0$ and $x < 0$ is the TMEI phase with $\phi_+ = (n_\phi + \frac{1}{2})\pi/\sqrt{2\pi}$. The fractional charge bound to the system end is calculated to be

$$q = e\sqrt{\frac{2}{\pi}}\int dx \partial_x \phi_+ = \left(n_\phi + \frac{1}{2}\right)e. \tag{14}$$

This half-quantized end charge thus confirms the bosonized theory with mirror-even excitonic orders as the TMEI phase.

On the other hand, we can also explore the Luther-Emery physics with $K_+ = \frac{1}{2}$, where the boson system can be reformulated into a noninteracting fermion theory. We focus on the bonding sector and rescale the bonding bosonic fields as $\phi_+/\sqrt{K_+} = \tilde{\phi}_+$ and $\sqrt{K_+}\theta_+ = \tilde{\theta}_+$. This allows us to introduce a set of new chiral fermion operators as $\tilde{\psi}_R = \frac{\eta_R}{\sqrt{4\pi a}} e^{i\sqrt{\pi}(\tilde{\phi}_+ + \tilde{\theta}_+)}$ and $\tilde{\psi}_L = \frac{\eta_L}{\sqrt{4\pi a}} e^{-i\sqrt{\pi}(\tilde{\phi}_+ - \tilde{\theta}_+)}$, which leads to the refermionized Hamiltonian

$$\mathcal{H}_+ = \int dx\ \tilde{\psi}^\dagger(-iv_+\gamma_z\partial_x + \alpha_1\gamma_x)\tilde{\psi}, \tag{15}$$

where $\tilde{\psi} = (\tilde{\psi}_R, \tilde{\psi}_L)^T$ is a spinor and $\gamma_{x,y,z}$ are Pauli matrices in the new chiral fermion basis. Crucially, Eq. (15) describes the low-energy theory of a massive Dirac fermion in one dimension. Since the vacuum condition pins $\phi_\pm = 0$ and is equivalent to $\alpha_1 < 0$, the interface between the vacuum and the double-wire forms a mass domain wall for the 1D Dirac fermion, which thus hosts a half-charge bound state. Therefore, Eq. (15) is exactly a fermionic model of the TMEI phase in the strongly interacting limit, which is consistent with the above bosonic analysis.

V. EXPERIMENTAL SIGNATURE

We now propose quantized transport signals in a four-terminal device to distinguish a trivial phase from the TMEI phase. As shown in Fig. 1, the four metallic electrodes (labeled $i = 1, 2, 3, 4$) are attached to the two-nanowire system. By applying a voltage drop and measuring the corresponding electric current, the conductance G_{ij} between lead i and lead j can feasibly be identified. The intrawire two-terminal conductance $G_{1,3}$ (or equivalently $G_{2,4}$) measures the electron tunneling probability across the system. Thus, $G_{1,3}$ is expected to show a U-shape dip as a function of the voltage bias because of the energy gap.

The nonlocal interwire conductance $G_{1,2}$ (or $G_{3,4}$) is the key to characterize TMEI physics. First, a nonzero $G_{1,2}$ has already implied strong interwire correlation effects, which could further clarify the excitonic nature of the energy gap measured in $G_{1,3}$. For a trivial system, we thus expect a similar conductance dip for $G_{1,2}$ due to the exciton gap. For the TMEI phase, however, its half-charge end mode will provide an additional resonant interwire conductance contribution to $G_{1,2}$:

$$\Delta G_{1,2} = \frac{e^2}{h}\frac{\Gamma^2}{\Gamma^2 + (\omega - E_0)^2}. \tag{16}$$

Here, E_0 is the energy of the half-charge mode and $\Gamma \sim m_0^2/v_F$ is the transport broadening. Thus, when the half-charge mode is in-gap, $G_{1,2}$ will show a quantized conductance peak of e^2/h as $\omega \to E_0$.

Numerical verifications of the above conductance patterns are performed using the Kwant PYTHON package [103]. Figures 4(a) and 4(c) and Figs. 4(b) and 4(d) show the conductance distributions as a function of the voltage bias for the topological trivial and nontrivial phases, respectively. In particular, Figs. 4(a) and 4(b) show an accidental chiral symmetry in their models, while Figs. 4(c) and 4(d) do not. Clearly, the conductance patterns behave exactly the same as predicted above. While every conductance displays a finite gap for the trivial system in Figs. 4(a) and 4(c), $G_{1,2}$ and $G_{3,4}$ for the TMEI phase show a quantized conductance peak when the energy of the lead electrons matches that of the localized end states, as shown in Figs. 4(b) and 4(d). Specifically, enforcing chiral symmetry in the system will lead to a zero-bias peak in Fig. 4(b). However, a general TMEI system that lacks chiral symmetry would display a peak at a finite voltage bias,

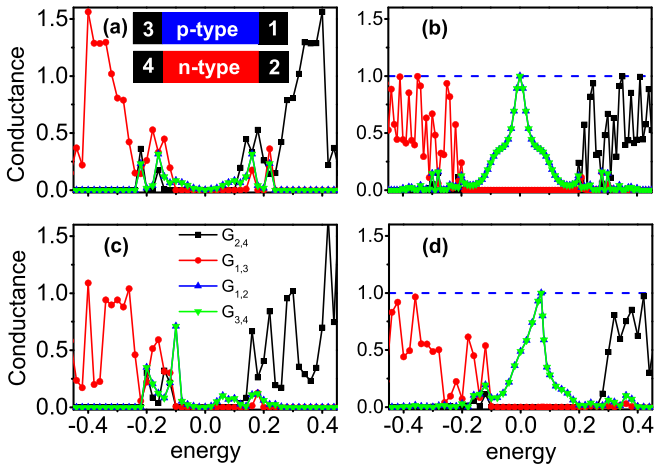

FIG. 4. Transport conductance $G_{i,j}$ in units of e^2/h between leads. In (a, c) trivial and (b, d) topological phases, the bulk is fully gapped, whereas the quantized $G_{1,2}$ and $G_{3,4}$ identify the half-charge end modes in the topological mirror excitonic phase. Resonant quantization occurs when the energy goes to 0 in (b) but at a finite energy in (d), due to the breaking of chiral symmetry. Parameters used are $m_0 = 1$, $v = 1$, $\delta\mu = 0$, $\mu = 0$, and $\Delta_0 = 0.2$ in (a)–(d); $\delta m = 0$ in (a) and (b) and $\delta m = 0.1$ in (c) and (d); and $h = 0.1$ in (a) and (c) and $h = 0.4$ in (b) and (d). The barrier potential between leads and nanowires is $V_0 = 1.5m_0$.

as shown in Fig. 4(d). Through the slight evolution from the free fermion limit with $K_\pm = 1$ to the interacting case with $K_\pm \neq 1$, the bulk energy gap of the system does not close. Therefore, we expect that our transport results in the mean-field limit will hold for an interacting TMEI phase.

VI. DISCUSSION AND CONCLUSIONS

Next, let us discuss the half-filling case, where one needs to consider the Umklapp scattering:

$$H_{\rm Um} \sim \alpha_3 \int dx\ \cos(2\sqrt{2\pi}\phi_-). \tag{17}$$

Therefore, the full boson Hamiltonian is

$$\begin{aligned}\mathcal{H} = \frac{v_\pm}{2}\int dx \left\{\frac{1}{K_\pm}(\partial_x\phi_\pm)^2 + K_\pm(\partial_x\theta_\pm)^2\right\} \\ + [\alpha_1\cos(2\sqrt{2\pi}\phi_+) + \alpha_2\cos(2\sqrt{2\pi}\theta_-) \\ + \alpha_3\cos(2\sqrt{2\pi}\phi_-)].\end{aligned} \tag{18}$$

The scaling dimensions of the coupling constants α_1, α_2, and α_3 are

$$\Delta_{\rm sd}(\alpha_1) = K_+, \quad \Delta_{\rm sd}(\alpha_2) = \frac{1}{K_-}, \quad \Delta_{\rm sd}(\alpha_3) = K_-. \tag{19}$$

When $K_\pm < 1$, we find $\Delta_{\rm sd}(\alpha_1) < 1$, $\Delta_{\rm sd}(\alpha_2) > 1$, and $\Delta_{\rm sd}(\alpha_3) < 1$. Namely, α_1 and α_3 are relevant under the RG and tend to flow to the strong-coupling limit. Consider the "semiclassical" limit with $\alpha_{1,3} \to +\infty$; $\phi_\pm$ are pinned to classical values with $\phi_\pm = (n_\pm + 1/2)\sqrt{\pi/2}$. Here $n_\pm \in \mathbb{Z}$ are integer-valued operators. As a result, the system develops an energy gap to all of its fermionic excitations. To understand the nature of this gapped phase, we define the following density-wave (dw) order parameters [95]:

$$\begin{aligned}\Delta^{(1)}_{\rm dw} &\sim \langle\Psi^\dagger_{e,R}\Psi_{e,L}\rangle \sim \langle e^{-2i\sqrt{\pi}\phi_e}\rangle \neq 0, \\ \Delta^{(2)}_{\rm dw} &\sim \langle\Psi^\dagger_{h,R}\Psi_{h,L}\rangle \sim \langle e^{-2i\sqrt{\pi}\phi_h}\rangle \neq 0.\end{aligned} \tag{20}$$

Therefore, we note that density-wave orders $\Delta^{(1,2)}_{\rm dw}$ develop nonzero expectation values directly, which implies the spontaneous breaking of the translational symmetry. Clearly, the mirror symmetry is spontaneously broken when the ϕ_- field is pinned. In this case, the density-wave phase is trivial in terms of the mirror-protected topology, simply because it is defined by a pinned ϕ_-.

Furthermore, let us briefly discuss how to realize the TMEI phase in a *single* nanowire of rotation-protected Dirac semimetal (e.g., a Cd_3As_2 nanowire with fourfold rotational symmetry C_4). As pointed out in Ref. [82], applying a magnetic field along the wire will naturally drive a 1D band inversion between an electronlike band with angular momentum $J = -\frac{1}{2}$ and a holelike band with $J = \frac{3}{2}$. As a result, any single-particle tunneling from the electron band to the hole band is naturally forbidden by the C_4 symmetry. In particular, with both C_4 and spatial inversion $\mathcal{I}$ symmetry, the Dirac semimetal nanowire also possesses an out-of-plane mirror $M_z = C_2\mathcal{I}$ that can protect the exciton-induced band topology in a corresponding nanowire geometry. Thus, without the complexity of aligning two quantum wires and careful band engineering in our double-wire setup, a single Dirac semimetal nanowire naturally fulfills all the symmetry and topological requisites for TMEI physics.

To summarize, we propose a new type of interacting crystalline topological state, the TMEI phase, that can be realized in Rashba nanowires and Dirac semimetal nanowires. In particular, we have established a bosonized theory to show the robustness of the TMEI phase beyond the mean-field approximation. This idea of exciton-induced crystalline topological states also has interesting higher-dimensional generalizations. For example, let us consider a bilayer 2D system with the top (bottom) layer contributing an electron (a hole) band near the Fermi level. An out-of-plane mirror symmetry M_z in this system can protect a TMEI phase with $|n_M|$ pairs of counter-propagating 1D edge modes, where $n_M \in \mathbb{Z}$ is the mirror Chern number for the system. On the other hand, when the bilayer system possesses in-plane mirror symmetry M_x and M_y, it is also possible to realize a higher-order TI with a quantized bulk quadruple moment and corner-localized charges. This is exactly an interacting and excitonic version of the electronic quadruple insulator in Refs. [104] and [105]. Detailed discussions of these 2D interacting crystalline topological systems are left for future work. We note that long-range excitonic orders may be realized in a 1D solid-state electron system [106]. It will be interesting to find the TMEI by numerical simulation, which is left for future work.

ACKNOWLEDGMENTS

R.-X.Z. acknowledges Yang-Zhi Chou for helpful discussion. L.-H.H. and C.W. were supported by AFOSR Grant No. FA9550-14-1-0168. R.-X.Z. was supported by a JQI Postdoctoral Fellowship. F.-C.Z. was supported by the Strategic

Priority Research Program of the Chinese Academy of Sciences (Grant No. XDB28000000), Beijing Municipal Science & Technology Commission (Grant No. Z181100004218001), National Science Foundation of China (Grant No.11674278), and National Basic Research Program of China (Grant No. 2014CB921203).

[1] M. Z. Hasan and C. L. Kane, Rev. Mod. Phys. **82**, 3045 (2010).
[2] X.-L. Qi and S.-C. Zhang, Rev. Mod. Phys. **83**, 1057 (2011).
[3] M. Z. Hasan and J. E. Moore, Annu. Rev. Condens. Matter Phys. **2**, 55 (2011).
[4] M. König, H. Buhmann, L. W. Molenkamp, T. Hughes, C.-X. Liu, X.-L. Qi, and S.-C. Zhang, J. Phys. Soc. Jpn. **77**, 031007 (2008).
[5] J. Maciejko, T. L. Hughes, and S.-C. Zhang, Annu. Rev. Condens. Matter Phys. **2**, 31 (2011).
[6] H. Zhang and S.-C. Zhang, Phys. Status Solidi (RRL) **7**, 72 (2013).
[7] T. Wehling, A. M. Black-Schaffer, and A. V. Balatsky, Adv. Phys. **63**, 1 (2014).
[8] B. Yan and S.-C. Zhang, Rep. Prog. Phys. **75**, 096501 (2012).
[9] Y. Ren, Z. Qiao, and Q. Niu, Rep. Prog. Phys. **79**, 066501 (2016).
[10] V. Galitski and I. B. Spielman, Nature **494**, 49 (2013).
[11] N. Goldman, G. Juzeliūnas, P. Öhberg, and I. B. Spielman, Rep. Prog. Phys. **77**, 126401 (2014).
[12] A. Bansil, H. Lin, and T. Das, Rev. Mod. Phys. **88**, 021004 (2016).
[13] C.-K. Chiu, J. C. Y. Teo, A. P. Schnyder, and S. Ryu, Rev. Mod. Phys. **88**, 035005 (2016).
[14] N. R. Cooper, J. Dalibard, and I. B. Spielman, Rev. Mod. Phys. **91**, 015005 (2019).
[15] M. König, S. Wiedmann, C. Brüne, A. Roth, H. Buhmann, L. W. Molenkamp, X.-L. Qi, and S.-C. Zhang, Science **318**, 766 (2007).
[16] I. Knez, R.-R. Du, and G. Sullivan, Phys. Rev. Lett. **109**, 186603 (2012).
[17] Y. Chen, J. G. Analytis, J.-H. Chu, Z. Liu, S.-K. Mo, X.-L. Qi, H. Zhang, D. Lu, X. Dai, Z. Fang *et al.*, Science **325**, 178 (2009).
[18] S. Wu, V. Fatemi, Q. D. Gibson, K. Watanabe, T. Taniguchi, R. J. Cava, and P. Jarillo-Herrero, Science **359**, 76 (2018).
[19] B. A. Bernevig and T. L. Hughes, *Topological Insulators and Topological Superconductors* (Princeton University Press, Princeton, NJ, 2013).
[20] M. Franz and L. Molenkamp, *Topological Insulators*, Vol. 6 (Elsevier, Amsterdam, 2013).
[21] S.-Q. Shen, *Topological Insulators*, Vol. 174 (Springer, Berlin, 2012).
[22] X. Chen, Z.-C. Gu, Z.-X. Liu, and X.-G. Wen, Science **338**, 1604 (2012).
[23] L. Fu, Phys. Rev. Lett. **106**, 106802 (2011).
[24] C. Fang, M. J. Gilbert, and B. A. Bernevig, Phys. Rev. B **86**, 115112 (2012).
[25] R.-J. Slager, A. Mesaros, V. Juričić, and J. Zaanen, Nat. Phys. **9**, 98 (2013).
[26] C.-X. Liu, R.-X. Zhang, and B. K. Van Leeuwen, Phys. Rev. B **90**, 085304 (2014).
[27] Z. Wang, Y. Sun, X.-Q. Chen, C. Franchini, G. Xu, H. Weng, X. Dai, and Z. Fang, Phys. Rev. B **85**, 195320 (2012).
[28] N. P. Armitage, E. J. Mele, and A. Vishwanath, Rev. Mod. Phys. **90**, 015001 (2018).
[29] R. S. K. Mong, A. M. Essin, and J. E. Moore, Phys. Rev. B **81**, 245209 (2010).
[30] C. Fang, M. J. Gilbert, and B. A. Bernevig, Phys. Rev. B **88**, 085406 (2013).
[31] R.-X. Zhang and C.-X. Liu, Phys. Rev. B **91**, 115317 (2015).
[32] S. Xu and C. Wu, Phys. Rev. Lett. **120**, 096401 (2018).
[33] T. Morimoto, H. C. Po, and A. Vishwanath, Phys. Rev. B **95**, 195155 (2017).
[34] T. H. Hsieh, H. Lin, J. Liu, W. Duan, A. Bansil, and L. Fu, Nat. Commun. **3**, 982 (2012).
[35] P. Dziawa, B. Kowalski, K. Dybko, R. Buczko, A. Szczerbakow, M. Szot, E. Łusakowska, T. Balasubramanian, B. M. Wojek, M. Berntsen *et al.*, Nat. Mater. **11**, 1023 (2012).
[36] Z. Wang, A. Alexandradinata, R. J. Cava, and B. A. Bernevig, Nature **532**, 189 (2016).
[37] J. Ma, C. Yi, B. Lv, Z. Wang, S. Nie, L. Wang, L. Kong, Y. Huang, P. Richard, P. Zhang *et al.*, Sci. Adv. **3**, e1602415 (2017).
[38] D. Zhang, M. Shi, T. Zhu, D. Xing, H. Zhang, and J. Wang, Phys. Rev. Lett. **122**, 206401 (2019).
[39] M. M. Otrokov, I. I. Klimovskikh, H. Bentmann, D. Estyunin, A. Zeugner, Z. S. Aliev, S. Gaß, A. U. B. Wolter, A. V. Koroleva, A. M. Shikin *et al.*, Nature **576**, 416 (2019).
[40] J. Li, Y. Li, S. Du, Z. Wang, B.-L. Gu, S.-C. Zhang, K. He, W. Duan, and Y. Xu, Sci. Adv. **5**, eaaw5685 (2019).
[41] Y. Gong, J. Guo, J. Li, K. Zhu, M. Liao, X. Liu, Q. Zhang, L. Gu, L. Tang, X. Feng, D. Zhang, W. Li, C. Song, L. Wang, P. Yu, X. Chen, Y. Wang, H. Yao, W. Duan, Y. Xu, S.-C. Zhang, X. Ma, Q.-K. Xue, and K. He, Chin. Phys. Lett. **36**, 076801 (2019).
[42] H. Li, S.-Y. Gao, S.-F. Duan, Y.-F. Xu, K.-J. Zhu, S.-J. Tian, J.-C. Gao, W.-H. Fan, Z.-C. Rao, J.-R. Huang *et al.*, Phys. Rev. X **9**, 041039 (2019).
[43] Y.-J. Hao, P. Liu, Y. Feng, X.-M. Ma, E. F. Schwier, M. Arita, S. Kumar, C. Hu, R. Lu, M. Zeng *et al.*, Phys. Rev. X **9**, 041038 (2019).
[44] Y. J. Chen, L. X. Xu, J. H. Li, Y. W. Li, H. Y. Wang, C. F. Zhang, H. Li, Y. Wu, A. J. Liang, C. Chen, S. W. Jung *et al.*, Phys. Rev. X **9**, 041040 (2019).
[45] R.-X. Zhang, F. Wu, and S. D. Sarma, Phys. Rev. Lett. **124**, 136407 (2020).
[46] M. Hohenadler and F. F. Assaad, J. Phys.: Condens. Matter **25**, 143201 (2013).
[47] T. Senthil, Annu. Rev. Condens. Matter Phys. **6**, 299 (2015).
[48] S. Rachel, Rep. Prog. Phys. **81**, 116501 (2018).
[49] C. Wu, B. A. Bernevig, and S.-C. Zhang, Phys. Rev. Lett. **96**, 106401 (2006).
[50] C. Xu and J. E. Moore, Phys. Rev. B **73**, 045322 (2006).
[51] S. Rachel and K. Le Hur, Phys. Rev. B **82**, 075106 (2010).
[52] D. Zheng, G.-M. Zhang, and C. Wu, Phys. Rev. B **84**, 205121 (2011).

[53] L. Fidkowski and A. Kitaev, Phys. Rev. B **81**, 134509 (2010).
[54] L. Fidkowski and A. Kitaev, Phys. Rev. B **83**, 075103 (2011).
[55] S. Ryu and S.-C. Zhang, Phys. Rev. B **85**, 245132 (2012).
[56] X.-L. Qi, New J. Phys. **15**, 065002 (2013).
[57] H. Yao and S. Ryu, Phys. Rev. B **88**, 064507 (2013).
[58] J. Wen, A. Rüegg, C.-C. J. Wang, and G. A. Fiete, Phys. Rev. B **82**, 075125 (2010).
[59] D. Pesin and L. Balents, Nat. Phys. **6**, 376 (2010).
[60] T. Neupert, L. Santos, C. Chamon, and C. Mudry, Phys. Rev. Lett. **106**, 236804 (2011).
[61] K. Sun, Z. Gu, H. Katsura, and S. Das Sarma, Phys. Rev. Lett. **106**, 236803 (2011).
[62] E. Tang, J.-W. Mei, and X.-G. Wen, Phys. Rev. Lett. **106**, 236802 (2011).
[63] J. C. Budich, R. Thomale, G. Li, M. Laubach, and S.-C. Zhang, Phys. Rev. B **86**, 201407(R) (2012).
[64] L. Wang, X. Dai, and X. Xie, Europhys. Lett. **98**, 57001 (2012).
[65] D. Cocks, P. P. Orth, S. Rachel, M. Buchhold, K. Le Hur, and W. Hofstetter, Phys. Rev. Lett. **109**, 205303 (2012).
[66] Z.-C. Gu and M. Levin, Phys. Rev. B **89**, 201113(R) (2014).
[67] C. Wang and T. Senthil, Phys. Rev. B **89**, 195124 (2014).
[68] Y.-Z. You and C. Xu, Phys. Rev. B **90**, 245120 (2014).
[69] Z. Bi, R. Zhang, Y.-Z. You, A. Young, L. Balents, C.-X. Liu, and C. Xu, Phys. Rev. Lett. **118**, 126801 (2017).
[70] M. Dzero, K. Sun, V. Galitski, and P. Coleman, Phys. Rev. Lett. **104**, 106408 (2010).
[71] A. Rüegg and G. A. Fiete, Phys. Rev. B **84**, 201103(R) (2011).
[72] T. Li, P. Wang, H. Fu, L. Du, K. A. Schreiber, X. Mu, X. Liu, G. Sullivan, G. A. Csáthy, X. Lin, and R.-R. Du, Phys. Rev. Lett. **115**, 136804 (2015).
[73] L. Du, X. Li, W. Lou, G. Sullivan, K. Chang, J. Kono, and R.-R. Du, Nat. Commun. **8**, 1971 (2017).
[74] R.-X. Zhang and C.-X. Liu, Phys. Rev. Lett. **118**, 216803 (2017).
[75] D. Xiao, C.-X. Liu, N. Samarth, and L.-H. Hu, Phys. Rev. Lett. **122**, 186802 (2019).
[76] S. de Léséleuc, V. Lienhard, P. Scholl, D. Barredo, S. Weber, N. Lang, H. P. Büchler, T. Lahaye, and A. Browaeys, Science **365**, 775 (2019).
[77] A. M. Morales and C. M. Lieber, Science **279**, 208 (1998).
[78] *Semiconductor Spintronics and Quantum Computation*, edited by D. D. Awschalom, D. Loss, and N. Samarth (Springer-Verlag, Berlin, Heidelberg, 2002).
[79] L. J. Lauhon, M. S. Gudiksen, D. Wang, and C. M. Lieber, Nature **420**, 57 (2002).
[80] C.-Z. Li, L.-X. Wang, H. Liu, J. Wang, Z.-M. Liao, and D.-P. Yu, Nat. Commun. **6**, 10137 (2015).
[81] L.-X. Wang, C.-Z. Li, D.-P. Yu, and Z.-M. Liao, Nat. Commun. **7**, 10769 (2016).
[82] R.-X. Zhang and C.-X. Liu, Phys. Rev. Lett. **120**, 156802 (2018).
[83] J.-J. Su and A. H. MacDonald, Nat. Phys. **4**, 799 (2008).
[84] R. Winkler, *Spin-Orbit Coupling Effects in Two-Dimensional Electron and Hole Systems*, Vol. 191 (Springer Science & Business Media, New York, 2003).
[85] C. E. Pryor and M.-E. Pistol, Phys. Rev. B **72**, 205311 (2005).
[86] We note that $i\sigma_x\tau_z$ also acts like a mirror operation to Eq. (1). However, we can explicitly break this accidental symmetry by turning on a small interwire tunneling term, $t\tau_x$, which respects M_x.
[87] N. Hao, P. Zhang, J. Li, Z. Wang, W. Zhang, and Y. Wang, Phys. Rev. B **82**, 195324 (2010).
[88] N. Hao, P. Zhang, and Y. Wang, Phys. Rev. B **84**, 155447 (2011).
[89] J. C. Budich, B. Trauzettel, and P. Michetti, Phys. Rev. Lett. **112**, 146405 (2014).
[90] D. I. Pikulin and T. Hyart, Phys. Rev. Lett. **112**, 176403 (2014).
[91] K. Chen and R. Shindou, Phys. Rev. B **96**, 161101(R) (2017).
[92] J. Zak, Phys. Rev. Lett. **62**, 2747 (1989).
[93] R. Resta, Rev. Mod. Phys. **66**, 899 (1994).
[94] A. Lau and C. Ortix, Eur. Phys. J.: Spec. Top. **227**, 1309 (2018).
[95] C. Wu, W. V. Liu, and E. Fradkin, Phys. Rev. B **68**, 115104 (2003).
[96] C. Wu, Phys. Rev. Lett. **95**, 266404 (2005).
[97] J. Von Delft and H. Schoeller, Ann. Phys. **7**, 225 (1998).
[98] D. Sénéchal, in *Theoretical Methods for Strongly Correlated Electrons*, edited by D. Sénéchal, A.-M. Tremblay, and C. Bourbonnais (Springer, Berlin, 2004), pp. 139–186.
[99] T. Giamarchi, *Quantum Physics in One Dimension*, Vol. 121 (Clarendon Press, Oxford, UK, 2003).
[100] R.-X. Zhang, C. Xu, and C.-X. Liu, Phys. Rev. B **94**, 235128 (2016).
[101] L. Fidkowski, R. M. Lutchyn, C. Nayak, and M. P. A. Fisher, Phys. Rev. B **84**, 195436 (2011).
[102] M. Cheng and H.-H. Tu, Phys. Rev. B **84**, 094503 (2011).
[103] C. W. Groth, M. Wimmer, A. R. Akhmerov, and X. Waintal, New J. Phys. **16**, 063065 (2014).
[104] W. A. Benalcazar, B. A. Bernevig, and T. L. Hughes, Science **357**, 61 (2017).
[105] C. W. Peterson, W. A. Benalcazar, T. L. Hughes, and G. Bahl, Nature **555**, 346 (2018).
[106] A. Kantian and D. S. L. Abergel, Phys. Rev. Lett. **119**, 037601 (2017).